

The ballooning structure of small edge localized modes in AUG and TCV

G.F. Harrer¹, E. Wolfrum², M.G. Dunne², T. Eich², R. Fischer², M. Griener², P. Hennequin³, A. Bock², B. Labit⁴, P. Manz², H. Meyer⁵, L. Radovanovic¹, S. Saarelma⁵, M. Willensdorfer², F. Aumayr¹, the ASDEX Upgrade Team² and the Eurofusion MST1 Team⁶

¹ *Institute of Applied Physics, TU Wien, Fusion@ÖAW, Vienna, Austria*

² *Max Planck Institute for Plasma Physics, Garching, Germany*

³ *Laboratoire de Physique des Plasmas, CNRS, Ecole Polytechnique, Palaiseau, France*

⁴ *Swiss Plasma Center, EPFL, Lausanne, Switzerland*

⁵ *CCFE, Culham Science Centre, Abingdon, Oxon, United Kingdom*

⁶ *see author list in B. Labit et al 2019 Nuclear Fusion 59 086020*

Introduction

In future fusion devices the collisionality $\nu_e^* \propto n_e/T_e^2$ at the pedestal top will be very low, $\nu_{e,\text{pedtop}}^* \sim 0.06$ [1], due to the expected high temperature. On the other hand at the very edge it should be high, $\nu_{e,\text{sep}}^* \sim 12$, because a high separatrix density is necessary for efficient power exhaust [2]. These conditions cannot be reached simultaneously in present-day machines. It is shown by the red shaded area in figure 1, that matching the ITER pedestal conditions in ASDEX Upgrade is only possible at low separatrix collisionality, whilst power exhaust experiments with high separatrix density and collisionality can only be achieved at high $\nu_{e,\text{pedestal}}^*$. This is a challenge for predictions about edge localized modes (ELMs) in ITER, as on the one hand, a lower pedestal top collisionality is predicted to cause larger, more severe type-I ELMs [1] and on the other hand, ASDEX Upgrade [3] and TCV [4] discharges with high separatrix collisionality, exhibit small Edge Localized Modes. These small ELMs and the effect of the magnetic shear on their ballooning stability, are the topic of this work.

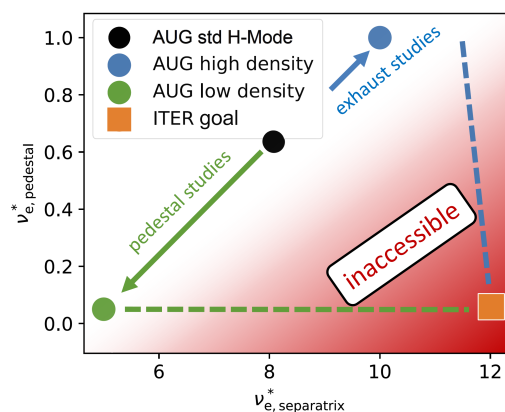


Figure 1: Electron collisionality operational space diagram: collisionality at the pedestal top as a function of separatrix collisionality

Small ELM scenarios

A phase where type-I ELMs dominate and one with small ELMs was chosen for the analysis of each machine. Figure 2 shows the reconstructed equilibria of the 4 analyzed time windows that were calculated on AUG with IDE [6] and on TCV with LIUQE. The orange shapes represent the small ELM dominant, whilst the blue show the type-I ELM dominant phases. The small ELM scenario is achieved in AUG by a plasma shape that is close to the double null configuration and in TCV by a high upper triangularity of 0.6. In the experiment, large type-I ELMs and small ELMs often coexist. This can be seen in figure 3, that shows ELM Monitor signals (upper row) and the plasma stored energy (lower row) of the 4 time windows.

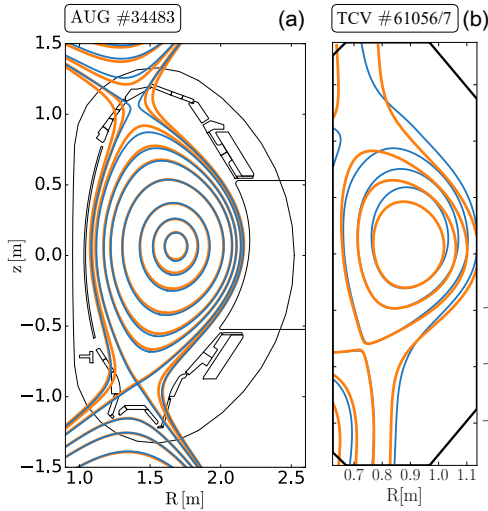


Figure 2: In (a) AUG discharge 34483: orange close to double null shape (small ELM dominant), blue, reduced elongation (type-I ELM dominant) and in (b): TCV discharges 61056 (orange, high delta small ELMs) and 61057 (blue, lower delta type-I ELM dominant).

These modes are driven by the pressure gradient close to the separatrix. It was shown by IPED stability calculations, that a flatter density gradient at the separatrix, leads to a shift of the peeling ballooning boundary, that describes type-I stability. Therefore small ELMs as local ballooning modes, could influence type-I ELM stability if they flatten the local density gradient. However ballooning modes are stabilized by magnetic shear. It was shown in [3, 4], that the flux surface average "global" magnetic shear $s \propto \frac{q'}{q}$ is different for cases comparing small ELMs to type-I

Figures 3 (a), (b), (e) and (f) show the AUG discharge # 34483 while (c), (d), (g) and (h) depict the two different TCV discharges (# 61056 & # 61057). The coexistence of the two ELM types is best seen in the two AUG phases where small ELMs (a,e) cause drops in the stored energy of less than 20kJ while the type-I ELMs (b,f) energy loss is around 10%. AUG data shows, that type-I ELMs and small ELMs coexist. Small ELMs dominate the signals for the first time window (around 3.5s) while the second time window contains some type-I ELMs again (see the big drops in W_{MHD} in figure 3 (f)).

The stabilizing effect of the magnetic shear

Recently, on ASDEX Upgrade, separatrix conditions have been linked to ballooning stability [5]. In [3], a model was proposed, that describes small ELMs as local high n ballooning modes. These

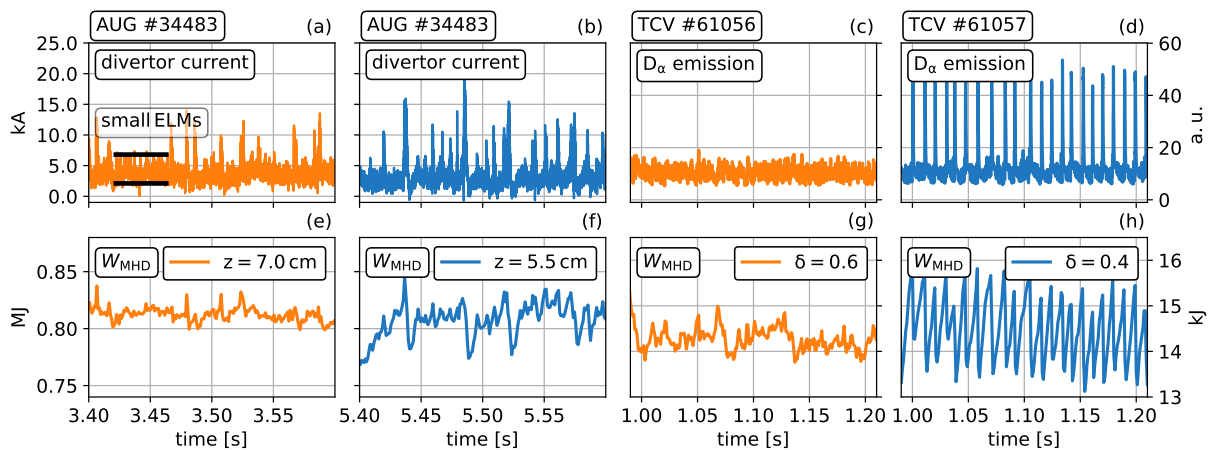


Figure 3: Time traces of three plasma discharges divided into small ELM dominant (orange) and type-I ELM dominant (blue) phases. The upper row shows ELM monitor signals, where (a) & (b) is the divertor current measured by shunts in the outer tiles of AUG. (c) & (d) show the D_α light as a typical ELM monitor in the two TCV discharges. The lower row (e)-(h) shows the plasma stored energy W_{MHD} , calculated from the equilibrium reconstruction.

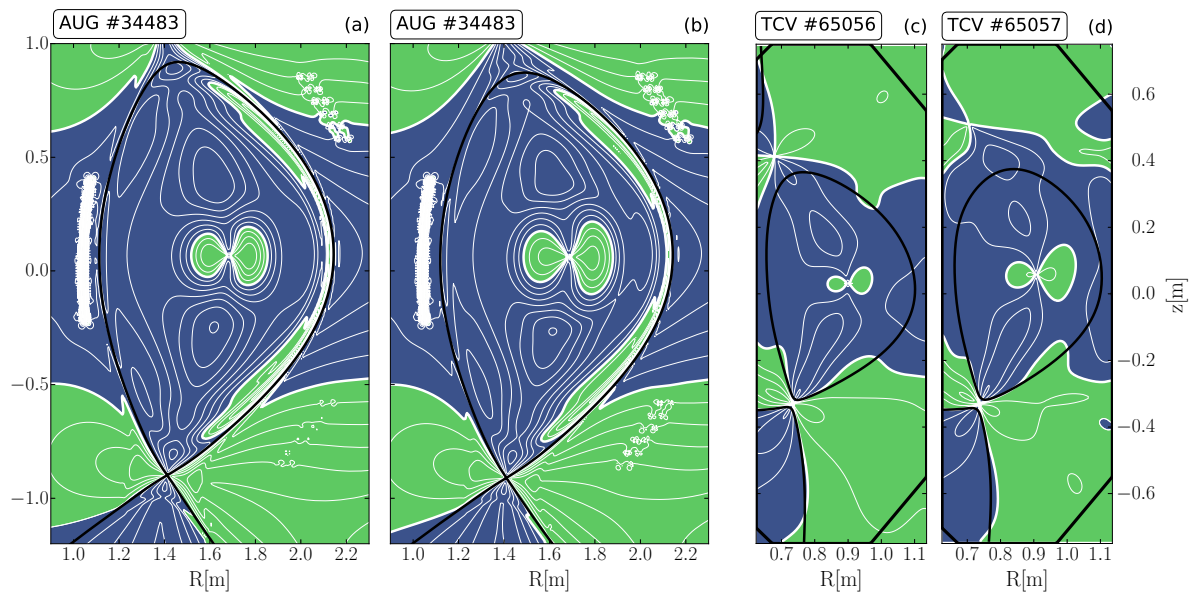


Figure 4: Local magnetic shear as defined in [7]. The green and blue color represent positive and negative shear while the white lines show contours of equal S_l . (a) and (c) represent the small ELM phases and (b) as well as (d), the phases where type-I ELMs dominate.

ELM dominant phases, most notably very close to the separatrix.

For a better understanding of the shaping effects the local magnetic shear $S_l = -\mathbf{e}_\perp \cdot \nabla \times \mathbf{e}_\perp$ as defined in [7] was calculated. Here the unit vector \mathbf{e}_\perp is perpendicular to the local magnetic field direction and lies in the flux surface. S_l represents the tilt of neighbouring flux tubes. It's unit is [rad/m] and it therefore provides a tilting angle when integrated along a field line. Figure 4 shows the local magnetic shear for the 4 time windows. Here green represents positive shear and blue negative shear. The white lines represent contours of constant local shear while the black lines show the separatrix.

There are some prominent qualitative differences comparing the small and large ELM cases for AUG and TCV. First the bootstrap current in the pedestal region causes a small area of positive shear around the outboard midplane for ASDEX Upgrade (a,b) but not for TCV (c,d). This positive shear band inside the separatrix connects two areas above and below the midplane that also exhibit positive shear. For the small ELM AUG case (a) the distance between these two areas is larger than in the type-I ELM case. An area of positive shear crossing the separatrix at the upper right of the plasmas, can be found in the small ELM phases of AUG (a) and TCV (c) while this is not the case for the type-I phases (b) and (d). More quantitative analysis of the local magnetic shear as well as the combination of the local shear calculations with $E \times B$ shear will be the subject of future work.

Ballooning stability

To investigate why the slight downward shift of the plasma in AUG discharge #34483 leads to a return of the type-I ELM dominance, the ideal ballooning stability code HELENA was utilized [8].

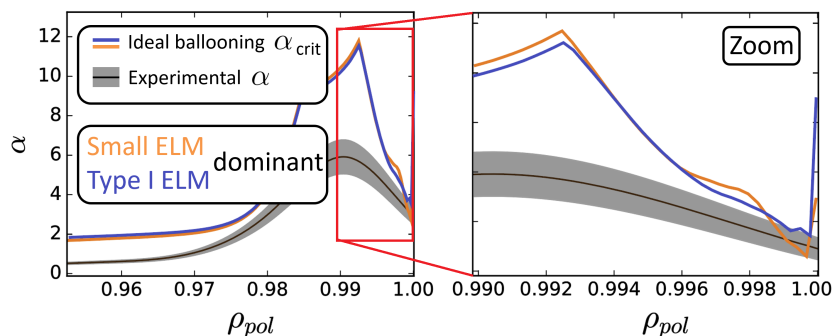


Figure 5: Normalized pressure gradient α vs normalized poloidal radius showing the ideal ballooning stability for AUG discharge 34483. The orange line represents the critical pressure gradient for the small ELM dominant phase, the blue line the phase with type-I ELMs

HELENA calculates the maximum possible normalized pressure gradient $\alpha \propto R_0 \frac{q^2}{B^2} \nabla p$ up to which the plasma is stable with respect to infinite- n ballooning modes. Figure 5 shows the results of such a ballooning stability calculation for AUG discharge 34483. The orange line represents the first time window marked in figure 3 (a), while the blue line represents the second investigated time window figure 3 (b). As the pressure profiles are very similar in both cases the experimental normalized pressure gradient shown with the shaded area does not change. As discussed in the previous section, the magnetic shear changes due to the downward shift of the plasma. This influences the critical alpha of the HELENA calculations. The experimental pressure gradient at the separatrix is very close to the stability limit in both cases. Comparing the zoomed windows on the right side of figure 5 shows, that for the small ELM dominant phase (orange) there is a region at around $\rho_{pol} = 0.999$ where the critical values cross the experimental data resulting in ballooning instability. After the downward shift of the plasma (blue) the critical α gradually rises and the radial region which is infinite- n ballooning unstable becomes smaller. This can be interpreted as further evidence, for the small ELMs being local ballooning modes that cause transport across the separatrix. The increased shear in the downward shifted plasma stabilizes the small ELMs and therefore leads to a return of the type-I ELMs.

Additional experiments are planned in the upcoming Eurofusion MST1 campaign, for a better understanding of additional properties, e.g. heating and fuelling dependence, of small ELM regimes.

Acknowledgement

This work has been carried out within the framework of the EUROfusion Consortium and has received funding from the Euratom research and training programme 2014-2018 and 2019-2020 under grant agreement No 633053. The views and opinions expressed herein do not necessarily reflect those of the European Commission. G. F. Harrer is a fellow of the Friedrich Schiedel Foundation for Energy Technology

References

- [1] A. Loarte et al. 2003 Plasma Physics and Controlled Fusion **45** 1549
- [2] M. Wischmeier et al. 2015 Journal of Nuclear Materials **463** 22-29
- [3] G.F. Harrer et al. 2018 Nuclear Fusion **58** 112001
- [4] B. Labit et al. 2019 Nuclear Fusion **59** 086020
- [5] T. Eich et al 2018 Nuclear Fusion **58** 034001
- [6] R. Fischer et al. 2016 Fusion Science and Technology **69** 526-536
- [7] P.J. Mc Carthy et al. 2013 Plasma Physics and Controlled Fusion **55** 085011
- [8] G.T.A Huysmans et al. 1991 Proceedings of Int. Conf. on Computational Physics p 371